



## Active harmonic filtering using current-controlled, grid-connected DG units with closed-loop power control

He, Jinwei; Li, Yun Wei; Blaabjerg, Frede; Wang, Xiongfei

*Published in:*

I E E E Transactions on Power Electronics

*DOI (link to publication from Publisher):*

[10.1109/TPEL.2013.2255895](https://doi.org/10.1109/TPEL.2013.2255895)

*Publication date:*

2014

*Document Version*

Early version, also known as pre-print

[Link to publication from Aalborg University](#)

*Citation for published version (APA):*

He, J., Li, Y. W., Blaabjerg, F., & Wang, X. (2014). Active harmonic filtering using current-controlled, grid-connected DG units with closed-loop power control. *I E E E Transactions on Power Electronics*, 29(2), 642-653. <https://doi.org/10.1109/TPEL.2013.2255895>

### General rights

Copyright and moral rights for the publications made accessible in the public portal are retained by the authors and/or other copyright owners and it is a condition of accessing publications that users recognise and abide by the legal requirements associated with these rights.

- Users may download and print one copy of any publication from the public portal for the purpose of private study or research.
- You may not further distribute the material or use it for any profit-making activity or commercial gain
- You may freely distribute the URL identifying the publication in the public portal -

### Take down policy

If you believe that this document breaches copyright please contact us at [vbn@aub.aau.dk](mailto:vbn@aub.aau.dk) providing details, and we will remove access to the work immediately and investigate your claim.

# Active Harmonic Filtering Using Current Controlled Grid-Connected DG Units with Closed-Loop Power Control

Jinwei He, *Student Member, IEEE*, Yun Wei Li, *Senior Member, IEEE*,

Frede Blaabjerg, *Fellow, IEEE*, and Xiongfei Wang, *Student Member, IEEE*

**<sup>1</sup>Abstract**—The increasing application of nonlinear loads may cause distribution system power quality issues. In order to utilize DG unit interfacing converters to actively compensate harmonics, this paper proposes an enhanced current control approach, which seamlessly integrates system harmonic mitigation capabilities with the primary DG power generation function. As the proposed current controller has two well decoupled control branches to independently control fundamental and harmonic DG currents, local nonlinear load harmonic current detection and distribution system harmonic voltage detection are not necessary for the proposed harmonic compensation method. Moreover, a closed-loop power control scheme is employed to directly derive the fundamental current reference without using any phase locked loops (PLL). The proposed power control scheme effectively eliminates the impacts of steady-state fundamental current tracking errors in the DG units. Thus, an accurate power control is realized even when the harmonic compensation functions are activated. In addition, this paper also briefly discusses the performance of the proposed method when DG unit is connected to a grid with frequency deviation. Simulated and experimental results from a single-phase DG unit validate the correctness of the proposed methods.

**Index Terms**— Distributed generation, phase-locked loop (PLL), harmonic extraction, resonant controller, virtual impedance, active power filter, harmonic compensation.

## I. INTRODUCTION

Due to the growing importance of renewable energy based power generation, a large number of power electronics interfaced DG units have been installed in the low voltage power distribution systems [1]. It has been reported that the control of interfacing converters can introduce system resonance issues [2]. Moreover, the increasing presence of nonlinear loads, such as variable speed drives, light-emitting diode (LED) lamps, compact fluorescent lamps (CFL), etc., will further degrade distribution system power quality.

---

Part of the work in this paper has been presented at the Applied Power Electronics Conference and Exposition (APEC2013), Long Beach, California, USA.

Copyright © 2011 IEEE. Personal use of this material is permitted. However, permission to use this material for any other purposes must be obtained from the IEEE by sending a request to [pubs-permission@ieee.org](mailto:pubs-permission@ieee.org).

The authors are with the Department of Electrical and Computer Engineering, University of Alberta, Canada. (email: [hjinwei@ualberta.ca](mailto:hjinwei@ualberta.ca) and [yunwei.li@ualberta.ca](mailto:yunwei.li@ualberta.ca)) and Aalborg University, Denmark. (email: [fbl@et.aau.dk](mailto:fbl@et.aau.dk) and [xwa@et.aau.dk](mailto:xwa@et.aau.dk))

To compensate distribution system harmonic distortions, a number of active and passive filtering methods have been developed [3]. However, installing additionally filters is not very favorable due to cost concerns. Alternatively, distribution system power quality enhancement using flexible control of grid-connected DG units is becoming an interesting topic [5-12], where the ancillary harmonic compensation capability is integrated with the DG primary power generation function through modifying control references. This idea is especially attractive considering that the available power from backstage renewable energy resources is often lower than the power rating of DG interfacing converters.

For the local load harmonic current compensation methods as discussed in [5-12], an accurate detection of local load harmonic current is important. Various types of harmonic detection methods [4] have been presented, such as the Fourier transformation based detection method in [13], the detection scheme using instantaneous real and reactive power theory in [14], Second-Order Generalized Integrator (SOGI) in [15], and the delayed signal cancellation based detection in [32]. Nevertheless, harmonic extraction process substantially increases the computing load of DG unit controllers. For a cost effective DG unit with limited computing ability, complex harmonic extraction methods might not be acceptable. Alternatively, an interesting harmonic detection-less method was proposed in [16, 17]. It shows that the main grid current can be directly controlled to be sinusoidal, instead of regulating DG output current to absorb local load harmonics. In this scenario, local load current is essentially treated as a disturbance in the grid current regulation loop. It should be noted that DG system normally has smaller stability margin when the direct control of grid current is employed. In addition, for the shunt active harmonic filtering via point of connection (PoC) harmonic voltage detection (also named as resistive active power filter (R-APF) in [12, 23]), the control techniques in [16, 17] cannot be used. Alternatively, the recently proposed hybrid voltage and current control method (HCM) [30] also allows the compensation of local load harmonics without using any harmonic detection process, where the well understood droop control scheme [22] is adopted to regulate the output power of the DG unit. Further considering that droop control based DG unit often features slow power control dynamics [21] and current controlled DG units are more widely installed in the distribution system, developing a robust current control based harmonic compensation method without using any system harmonic detection is very necessary.

It is worth mentioning that the DG real and reactive power control performance shall not be affected during the harmonic compensation. To satisfy this requirement, the fundamental DG current reference shall be calculated according to power references. Conventionally, the fundamental current reference can be determined based on the assumption of ripple-free grid voltage with fixed magnitude, and the PLL is used to

synchronize the fundamental current reference with the main grid. However, considering that PoC voltage magnitude often varies due to the distribution system power flow fluctuations, this method may cause nontrivial power control errors. Alternatively, the fundamental current reference can also be calculated through the “power-current transformation” in [7], where only the detected PoC voltage fundamental component is used in the calculation. However, for a DG unit with the ancillary harmonic compensation capability, the interactions between distorted DG current and PoC harmonic voltages may contribute some DC real and reactive power bias [31], and these power bias cannot be directly addressed in the control method in [7]. In order to ensure accurate power tracking performance, a closed-loop DG power control is necessary.

To simplify the operation of DG units with ancillary harmonic compensation capabilities while maintaining accurate power control, this paper proposes an improved current controller with two parallel control branches. The first control branch is responsible for DG unit fundamental current control, and the second one is employed to compensate local load harmonic current or feeder resonance voltage. In contrast to the conventional control methods with harmonic detection, the PoC voltage and local load current can be directly used as the input of the proposed current controller, without affecting the harmonic compensation accuracy of the DG unit. Moreover, with simple PI regulation in the outer power control loop, the proposed DG unit also achieves zero steady-state power tracking errors even when the fundamental current tracking has some steady-state errors. Simulated and experimental results from a single-phase DG unit validate the effectiveness of the proposed DG control method.

## II. DG UNITS WITH HARMONIC COMPENSATION

In this section, a DG unit using the compensation strategies in the conventional active power filters is briefly discussed. Afterwards, a detailed discussion on the proposed control strategy is presented.

### A. Conventional local load harmonic current compensation

Fig. 1 illustrates the configuration of a single-phase DG system, where the interfacing converter is connected to the distribution system with a coupling choke ( $L_f$  and  $R_f$ ). There is a local load at PoC. In order to improve the power quality of grid current ( $I_2$ ), the harmonic components of local load current ( $I_{Local}$ ) shall be absorbed through DG current ( $I_1$ ) regulation.

The DG unit control scheme is illustrated in the lower part. As shown, its current reference consists of two parts. The first one is the fundamental current reference ( $I_{ref,f}$ ), which is synchronized with PoC voltage ( $V_{PoC}$ ) as

$$I_{ref,f} = \frac{(\cos(\theta) \cdot P_{ref} + \sin(\theta) \cdot Q_{ref})}{E^*} \quad (1)$$

where  $\theta$  is the PoC voltage phase angle detected by PLL,  $P_{ref}$  and  $Q_{ref}$  are the real and reactive power reference, and  $E^*$  is the nominal voltage magnitude of the system.

However, the current reference generator in (1) is not accurate in controlling DG power, due to variations of the PoC voltage magnitude. To overcome this drawback, an improved power control method with consideration of PoC voltage magnitude fluctuations [11] was developed as shown in the following of this subsection.

First, the fundamental PoC voltage  $V_{PoC\alpha_f}$  and its orthogonal component  $V_{PoC\beta_f}$  (quarter cycle delayed respect to  $V_{PoC\alpha_f}$ ) are obtained by using SOGI [15] as

$$V_{PoC\alpha_f} = \frac{2\omega_{D1}s}{s^2 + 2\omega_{D1}s + \omega_f^2} \cdot V_{PoC} \quad (2)$$

$$V_{PoC\beta_f} = \frac{2\omega_{D1}\omega_f}{s^2 + 2\omega_{D1}s + \omega_f^2} \cdot V_{PoC} \quad (3)$$

where  $\omega_{D1}$  is the cut-off bandwidth of SOGI and  $\omega_f$  is the fundamental angular frequency.

For a single-phase DG system, relationships between the power reference and the fundamental reference current can be established in the artificial stationary  $\alpha - \beta$  reference frame as shown in (4) and (5)

$$P_{ref} = 1/2 \cdot (V_{PoC\alpha_f} \cdot I_{ref\alpha_f} + V_{PoC\beta_f} \cdot I_{ref\beta_f}) \quad (4)$$

$$Q_{ref} = 1/2 \cdot (V_{PoC\beta_f} \cdot I_{ref\alpha_f} - V_{PoC\alpha_f} \cdot I_{ref\beta_f}) \quad (5)$$

where  $I_{ref\alpha_f}$  and  $I_{ref\beta_f}$  are the DG fundamental current reference and its orthogonal component in the artificial  $\alpha - \beta$  reference frame. Similarly,  $V_{PCC\alpha_f}$  and  $V_{PCC\beta_f}$  are PoC fundamental voltage and its orthogonal component. According to (4) and (5), the instantaneous fundamental current reference ( $I_{ref,f}$ ) of a single-phase DG unit can be obtained as

$$I_{ref,f} = I_{ref\alpha_f} = \frac{2(V_{PoC\alpha_f} \cdot P_{ref} + V_{PoC\beta_f} \cdot Q_{ref})}{V_{PoC\alpha_f}^2 + V_{PoC\beta_f}^2} \quad (6)$$

Moreover, to absorb the harmonic current of local nonlinear load, the DG harmonic current reference ( $I_{ref,h}$ ) is produced

$$I_{ref,h} = G_D(s) \cdot I_{Local} = \sum_{h=3,5,7,9,\dots} \frac{2\omega_{D2}s}{s^2 + 2\omega_{D2}s + \omega_h^2} \cdot I_{Local} \quad (7)$$

where  $G_D(s)$  is the transfer function of the harmonic extractor. To realize selective harmonic compensation performance [24, 25],  $G_D(s)$  is designed to have a set of band-pass filters with cutoff frequency  $\omega_{D2}$ .

With the derived fundamental and harmonic current references, the DG current reference is written as  $I_{ref} = I_{ref,f} + I_{ref,h}$ . Afterwards, the proportional and multiple resonant controllers [12, 18-20] are adopted to ensure rapid current tracking

$$V_{PWM}^* = G_{cur}(s) \cdot (I_{ref} - I_1) = (K_p + \sum_{h=f,3,5,\dots,15} \frac{2K_{ih}\omega_c s}{s^2 + 2\omega_c s + \omega_h^2}) \cdot (I_{ref,f} + I_{ref,h} - I_1) \quad (8)$$

where  $V_p^*$  is the reference voltage for pulse width modulation (PWM) processing.  $K_p$  is the proportional gain of the current controller  $G_{cur}(s)$ ,  $K_{ih}$  is the resonant controller gain at the order  $h$ ,  $\omega_c$  is the cutoff frequency of the resonant controller, and  $\omega_h$  is the angular frequency at fundamental and selected harmonic frequencies.

### B. Conventional feeder resonance voltage compensation

It should be pointed out that the objective of local load harmonic compensation is to ensure sinusoidal grid current  $I_2$

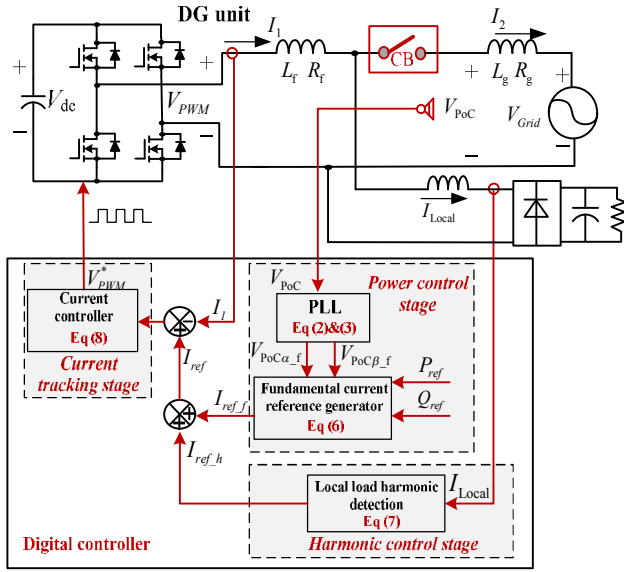


Fig.1. Diagram of a DG unit with local load harmonic current compensation capability.

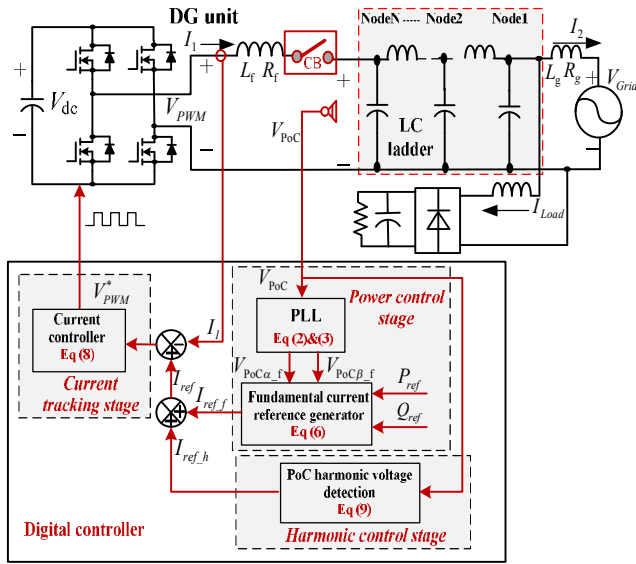


Fig.2. Diagram of a DG unit with PoC harmonic voltage mitigation capability.

in Fig. 1. In this control mode, DG unit should not actively regulate the PoC voltage quality. As a result, the PoC voltage can be distorted especially when it is connected to the main grid through a long underground cable with nontrivial parasitic capacitance [8, 23]. In this case, the feeder is often modeled by an LC ladder [23, 26]. To address the resonance issue associated with long underground cables, the R-APF concept can also be embedded in the DG unit current control as illustrated in Fig. 2. Compared to Fig.1, the DG harmonic current reference in this case is modified as

$$I_{ref\_h} = \left(-\frac{1}{R_v}\right) \cdot (G_D(s) \cdot V_{PoC}) \quad (9)$$

where  $R_v$  is the virtual damping resistance at harmonic frequencies. With this harmonic current reference (9), the DG unit essentially works as a small equivalent harmonic resistor at the end of the feeder, when it is viewed at power distribution system level [33-34]. By providing sufficient damping effects to the long feeder, the voltage quality at different positions of the feeder can be improved.

### C. Proposed harmonic compensation method

Note that for the local load harmonic current compensation and the PoC harmonic voltage compensation, the harmonic current is absorbed by the DG unit. Consequently, interactions between DG harmonic current and PoC harmonic voltage may cause some steady-state DG power offset [31]. Nevertheless, the power control using fundamental current reference in (6) is still in an open-loop manner, which can not address the power offset introduced by harmonics interactions. In order to achieve accurate power control performance in current controlled DG units, the instantaneous fundamental current reference (including both magnitude and phase angle information) can be determined by a simple closed-loop power control strategy as

$$I_{ref\_f} = g_1 \cdot V_{PoC\alpha} + g_2 \cdot V_{PoC\beta} \quad (10)$$

where  $V_{PoC\alpha}$  is the non-filtered PoC voltage expressed in the  $\alpha - \beta$  reference frame ( $V_{PoC\alpha} = V_{PoC}$ ) and  $V_{PoC\beta}$  is its orthogonal component. The gains  $g_1$  and  $g_2$  are adjustable and they are used to control DG unit real and reactive power, respectively. The detailed regulation law is shown in (11) and (12) as

$$g_1 = \left(k_{p1} + \frac{k_{i1}}{s}\right) \cdot \left(\frac{1}{\tau s + 1} \cdot P_{ref} - P_{DG}\right) + \frac{P_{ref}}{(E^*)^2} \quad (11)$$

$$g_2 = \left(k_{p2} + \frac{k_{i2}}{s}\right) \cdot \left(\frac{1}{\tau s + 1} \cdot Q_{ref} - Q_{DG}\right) + \frac{Q_{ref}}{(E^*)^2} \quad (12)$$

where  $k_{p1}$ ,  $k_{i1}$ ,  $k_{p2}$ ,  $k_{i2}$  are proportional and integral control parameters,  $P_{ref}$  and  $Q_{ref}$  are the real and reactive power references,  $E^*$  is the nominal voltage magnitude of the DG unit,  $\tau$  is the time constant of first-order low pass filters.  $P_{DG}$  and  $Q_{DG}$  are measured DG power with low pass filtering as

$$P_{DG} = \frac{1}{2(\tau s + 1)} \cdot (V_{PCC\alpha} \cdot I_{1\alpha} + V_{PCC\beta} \cdot I_{1\beta}) \quad (13)$$

$$Q_{DG} = \frac{1}{2(\tau s + 1)} \cdot (V_{PCC\beta} \cdot I_{1\alpha} - V_{PCC\alpha} \cdot I_{1\beta}) \quad (14)$$

where  $I_{1\alpha}$  is the non-filtered DG current expressed in the stationary  $\alpha - \beta$  frame ( $I_1 = I_{1\alpha}$ ) and  $I_{1\beta}$  is its delayed orthogonal component. Note that in (13) and (14), the power offset caused by harmonic voltage and harmonic current interactions is also considered.

Although the proposed closed-loop power control method eliminates power tracking errors, it can be seen that the fundamental current reference in (10) will be distorted if PoC voltage has some ripples. When it is applied to the current

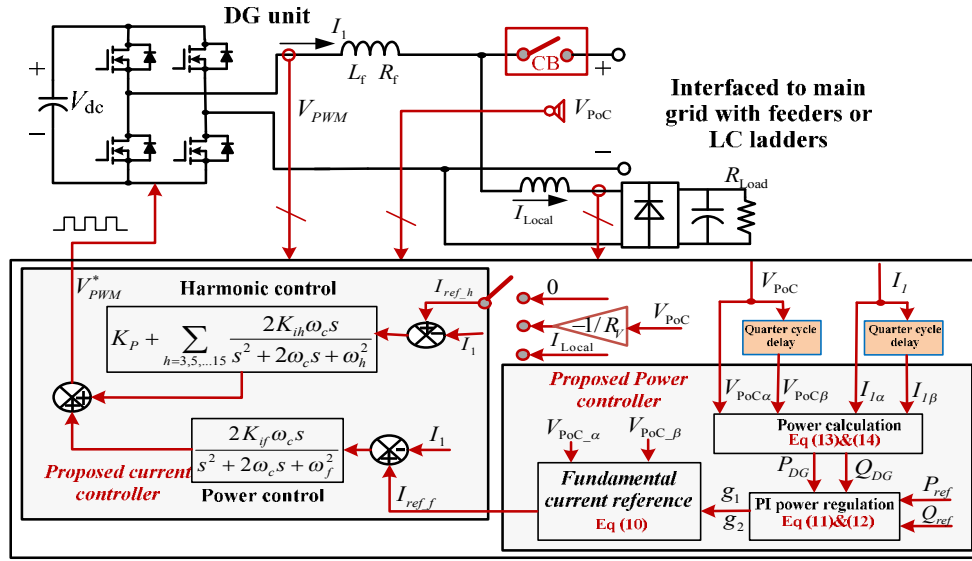


Fig. 3. Diagram of a DG unit with the proposed control scheme.

controller in (8), the distorted fundamental current reference will affect the performance of DG harmonic current tracking.

To overcome this drawback, an improved proportional and resonant controller with two control branches is proposed as

$$\begin{aligned}
 V_{PWM}^* &= \frac{\text{Branch1: power control}}{s^2 + 2\omega_c s + \omega_f^2} \cdot (I_{ref\_f} - I_1) \\
 &+ (K_p + \sum_{h=3,5,\dots,15} \frac{2K_{ih}\omega_c s}{s^2 + 2\omega_c s + \omega_h^2}) \cdot (I_{ref\_h} - I_1) \\
 &= \underset{\text{Branch1: power control}}{G_f(s)} \cdot (I_{ref\_f} - I_1) + \underset{\text{Branch2: harmonic control}}{G_h(s)} \cdot (I_{ref\_h} - I_1) \quad (15)
 \end{aligned}$$

As shown, the fundamental current reference in (10) is regulated by the “power control” branch in (15). As only fundamental resonant controller is adopted in this branch, the impacts of harmonic components in  $I_{ref\_f}$  can be automatically filtered out. Therefore, the power control branch will not introduce any obvious harmonic disturbances to the harmonic control branch in (15).

Meanwhile, the harmonic current reference  $I_{ref\_h}$  is regulated by the “harmonic control” branch, where only harmonic resonant controllers are included. Considering some non-characteristic harmonics exist the system, a small proportional gain  $K_p$  is used to ensure superior harmonic current tracking.

As fundamental resonant controller is not included in the harmonic control branch, it is possible to remove the harmonic extraction blocks in (7). Accordingly, the local load current or PoC voltage without any filtering is directly used as the input of the harmonic control branch. Note that when the harmonic current reference  $I_{ref\_h}$  is set to zero, the harmonic control branch ensures that the DG current is ripple-free. This is very similar to the performance of conventional DG unit without any compensation, where the DG unit current is controlled to be sinusoidal.

In summary, the harmonic current reference in (15) can have three options as given in (16)

$$I_{ref\_h} = \begin{cases} I_{Local} & \text{Local nonlinear load compensation} \\ -V_{PoC} / R_f & \text{Feeder resonance voltage compensation} \\ 0 & \text{DG harmonic current rejection} \end{cases} \quad (16)$$

With the proposed method in (15) and the control reference in (16), it seems there is a complication. When the local load current or the PoC voltage are directly employed as the input of the harmonic control branch (see (16)), the proportional gain  $K_p$  in (15) makes the output of harmonic control branch has some fundamental components. These fundamental components may cause interference with the power control branch. As a result, the fundamental current tracking will have steady-state errors. However, further considering that the fundamental current tracking in (15) essentially behaves as an inner loop of the proposed closed-loop DG power ( $P_{DG}$  and  $Q_{DG}$ ) regulation in (10), the DG unit still has zero steady-state power control error even when its fundamental current tracking has some errors.

The diagram of the proposed control method is presented in Fig. 3. It shows that the PLL and harmonic detection as shown in the conventional harmonic compensation schemes in (7) and (9) are removed from the proposed DG controller. Also an accurate real and reactive power control is guaranteed by two PI regulators in the power control loop.

It is important to mention that grid voltage frequency variations [35] often affect the power control accuracy and the harmonic compensation performance of the DG unit. As PI controllers are used in the closed loop power control in (11) and (12), zero steady-state power control error can still be realized even when grid voltage frequency has variations. On the other hand, to alleviate the impact of frequency variation to DG harmonic current tracking accuracy, wide bandwidth ( $\omega_c$ ) harmonic resonant controllers should be considered in (15). Additionally, if the DG unit needs to be connected to a utility grid with nontrivial frequency variations, a frequency estimator can be adopted to detect the frequency of the grid. In this case,

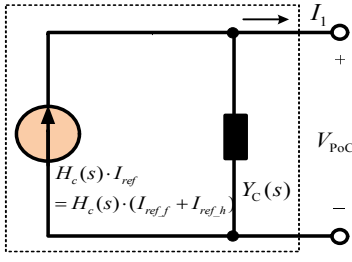


Fig. 4. Equivalent circuit of a DG unit using conventional current control method.

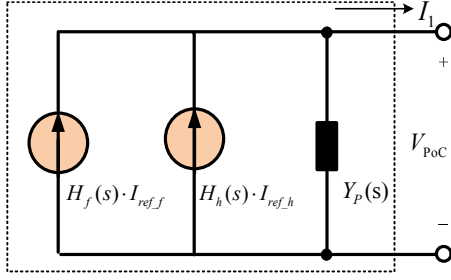


Fig. 5. Equivalent circuit of a DG unit using the proposed current control method.

the detected grid frequency is used as a parameter of resonant controllers and the DG current tracking accuracy can be improved accordingly. Note that the frequency detector, such as that in [36], is simpler than a PLL, as the grid angle calculation is not needed in the proposed DG power control loop.

### III. MODELING OF DG UNIT WITH THE PROPOSED CURRENT CONTROL SCHEME

In this section, the harmonic compensation performance using the proposed current controller is investigated.

#### A. Modeling of the proposed current control method

It is well understood that the current controlled inverter shall be described as a closed-loop Norton equivalent circuit [27, 29]

$$I_1 = H_c(s) \cdot I_{ref} - Y_c(s) \cdot V_{PoC} \quad (17)$$

where the gain ( $H_c(s)$  and  $Y_c(s)$ ) can be derived based on the conventional current controller in (8) and the DG unit circuitry parameters [27]. The corresponding equivalent circuit is shown in Fig. 4. Note that for the DG unit with harmonic compensation capability, the current reference  $I_{ref}$  in Fig. 4 has two components ( $I_{ref_f}$  and  $I_{ref_h}$ ).

For the DG unit using the proposed current control method, its equivalent circuit is derived as shown in the rest of this subsection.

First, (18) describes the transfer function of DG unit filter plant  $G_{ind}(s)$  as

$$\begin{aligned} I_1 &= G_{ind}(s) \cdot (V_{PWM} - V_{PoC}) \\ &= \frac{I}{L_f s + R_f} \cdot (V_{PWM} - V_{PoC}) \end{aligned} \quad (18)$$

where  $L_f$  is the inductance of the DG coupling choke and  $R_f$  is its stray resistance.  $V_{PWM}$  is the average inverter output voltage.

Additionally, the delay of DG control [28] is written as

$$V_{PWM} = e^{-1.5T_d \cdot s} \cdot V_{PWM}^* \quad (19),$$

where  $T_d$  is the sampling period of the system. Note that the delay here includes one sampling period processing delay and half sampling period voltage modulation delay.

By solving (15), (18), and (19), the closed-loop DG current response can be given as

$$I_1 = H_f(s) \cdot I_{ref_f} + H_h(s) \cdot I_{ref_h} - Y_p(s) \cdot V_{PoC} \quad (20)$$

where  $H_f(s)$  and  $H_h(s)$  represent the closed-loop response of DG unit current to fundamental and harmonic current references, respectively.  $Y_p(s)$  demonstrates the sensitivity of DG line current tracking to PoC voltage disturbances [27]. The detailed expression of terms in (20) is listed as

$$H_f(s) = \frac{e^{-1.5T_d \cdot s} \cdot G_f(s) \cdot G_{ind}(s)}{1 + e^{-1.5T_d \cdot s} \cdot (G_f(s) + G_h(s)) \cdot G_{ind}(s)},$$

$$H_h(s) = \frac{e^{-1.5T_d \cdot s} \cdot G_h(s) \cdot G_{ind}(s)}{1 + e^{-1.5T_d \cdot s} \cdot (G_f(s) + G_h(s)) \cdot G_{ind}(s)}, \text{ and}$$

$$Y_p(s) = \frac{G_{ind}(s)}{1 + e^{-1.5T_d \cdot s} \cdot (G_f(s) + G_h(s)) \cdot G_{ind}(s)}.$$

For the DG unit with the proposed current control scheme, a modified Norton equivalent circuit with two controlled current sources can be applied to demonstrate the unique behavior of the proposed controller. As illustrated in Fig. 5, the current source  $H_f(s)I_{ref_f}$  is responsible for regulating DG unit fundamental current. Additionally, the current source  $H_h(s)I_{ref_h}$  aims to compensate system harmonics at selected harmonic frequencies.

#### B. Bode plot analysis

The performance of a DG unit using conventional current control (8) and the proposed current control (15) are compared in this subsection.

The closed-loop response of DG current to fundamental current references is shown in Fig. 6. It can be seen that the proposed control method ( $H_f(s)$ ) gives 0 dB and 0 degree response at the fundamental frequency, and the magnitude response attenuates rapidly at selected harmonic frequencies. Therefore, the fundamental current reference  $I_{ref_f}$  in (15) is not necessarily to be harmonic free. While for the DG unit using the conventional current control in (8), the magnitude response ( $H_c(s)$ ) is close to 0 dB at the selected harmonic frequencies. Thus, any harmonic distortions in the fundamental current reference  $I_{ref_f}$  will bring disturbances to the DG harmonic current control.

Similarly, the response of the DG current to harmonic current reference  $I_{ref_h}$  in (15) is also given in Fig. 7. When the proposed method is applied to the DG unit, it is obvious that  $H_h(s)$  features low magnitude response at the fundamental frequency. On the other hand, as the conventional current control method in (8) couples fundamental and harmonic current reference together, the fundamental component in  $I_{ref_h}$

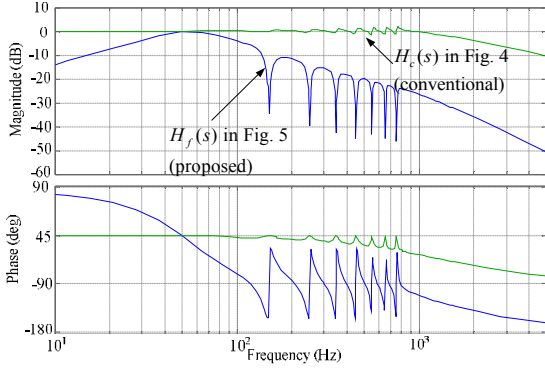


Fig. 6. Closed-loop response ( $H_C(s)$  and  $H_f(s)$ ) of a DG unit using conventional current control method in (8) and the proposed current control method in (15).

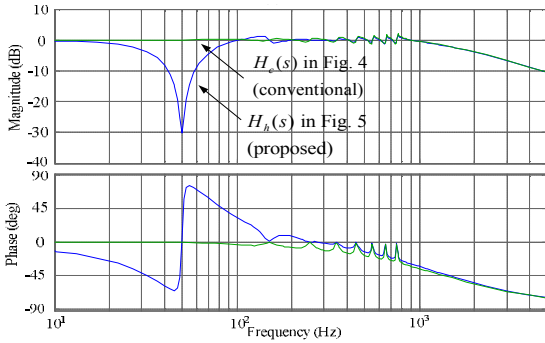


Fig. 7. Closed-loop response ( $H_C(s)$  and  $H_h(s)$ ) of a DG unit using conventional current control method in (8) and the proposed current control method in (15).

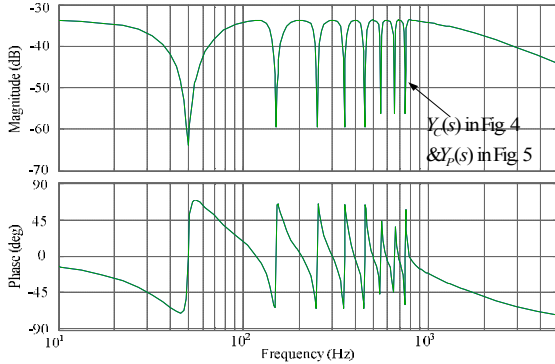


Fig. 8. Shunt admittance ( $Y_C(s)$  and  $Y_p(s)$ ) of a DG unit using conventional current control method in (8) and the proposed current control method in (15).

will cause more interference with the regulation of  $I_{ref}$ . As a result, harmonic detection is necessary for system harmonic compensation using conventional current control method.

The Bode plots of shunt admittance  $Y_p(s)$  and  $Y_C(s)$  are shown in Fig. 8. It can be seen that the shunt admittance have identical frequency domain response by using the conventional and the proposed methods. As these admittances have low magnitude response at the both fundamental and selected

TABLE I. PARAMETERS IN SIMULATION & EXPERIMENT

System Parameter	Value
Grid voltage	Simulation 230V/50Hz Experiment 115V/50Hz
DG filter	$L_f=6.5\text{mH}$ , $R_f=0.15\Omega$
Grid feeder	$L_g=3.4\text{mH}$ , $R_g=0.15\Omega$
LC ladder with five identical LC filter	$L=1.0\text{mH}$ , $C=25\mu\text{F}$ for each LC filter
Sampling/Switching frequency	20kHz/10kHz
DC link voltage	Simulation 550V Experiment 350V
<b>Power Control Parameter</b>	
Real power control $k_{p1}$ , $k_{i1}$	$k_{p1}=0.00001$ , $k_{i1}=0.001$
Reactive power control $k_{p2}$ , $k_{i2}$	$k_{p2}=0.00001$ , $k_{i2}=0.001$
LPF time constant $\tau$	0.0322 Sec
<b>Current control Parameter</b>	
Proportional gain $K_p$	48
Resonant gains $K_{ih}$	1500 ( $h=7$ ); 900 ( $h=3, 5, 7, 9$ ); 600 ( $h=11, 13, 15$ )
Resonant controller bandwidth $\omega_c$	4.1rad/s
$R_V$ (for PoC harmonic voltage compensation)	5 $\Omega$

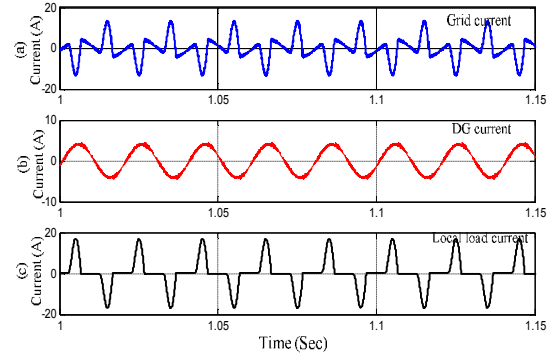


Fig. 9. Performance of the DG unit during DG harmonic rejection. (a: grid current  $I_2$ ; b: DG current  $I_1$ ; c: local load current  $I_{Local}$ .)

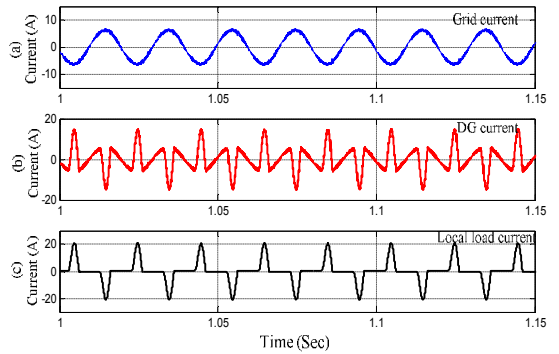


Fig. 10. Performance of the DG unit during local load compensation. (a: grid current  $I_2$ ; b: DG current  $I_1$ ; c: local load current  $I_{Local}$ .)

harmonic frequencies, PoC voltage disturbances only have minor impacts to DG current tracking.

#### IV. SIMULATED AND EXPERIMENTAL RESULTS

In order to verify the correctness of the proposed control strategy, simulated and experimental results are obtained from a single-phase DG unit.

##### A. Simulated results

- Compensation of local nonlinear loads

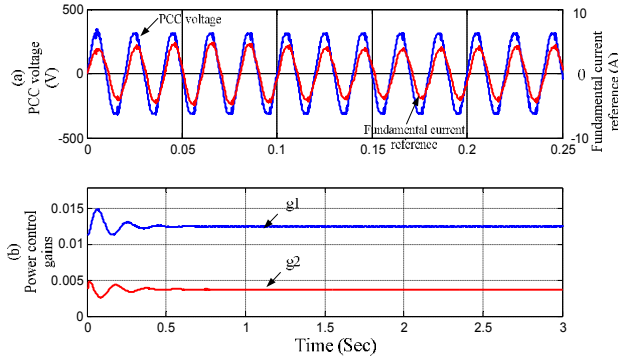


Fig. 11. Power control reference during local load harmonic compensation. (a: PoC voltage and fundamental current reference  $I_{ref\_f}$ , b: power control gains  $g_1$  and  $g_2$ ).

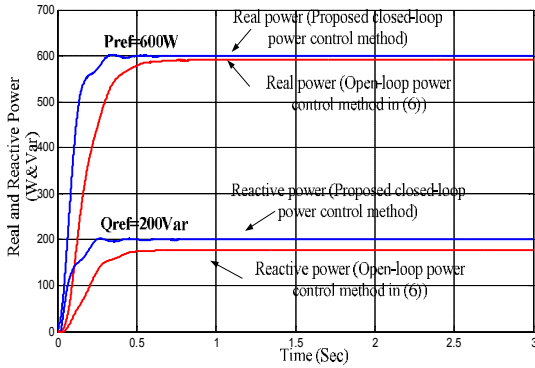


Fig.12. Power flow of the DG unit during local load harmonic current compensation. ( $P_{ref}=600W$  and  $Q_{ref}=200Var$ ).

First, the DG unit with a local diode rectifier load is tested in the simulation. The configuration of the system is the same as Fig. 1 and PoC is connected to a stiff controlled voltage source (to emulate the main grid) with nominal 50Hz frequency.

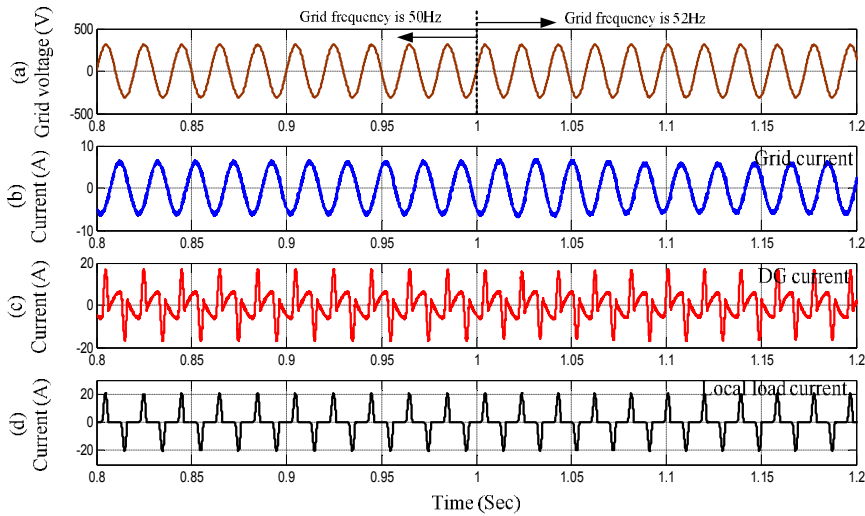


Fig.13. Performance of the DG unit under local harmonic compensation mode (2Hz grid voltage frequency change at 1.0 sec). (a: grid voltage  $V_{grid}$ ; b: grid current  $I_2$ ; c: DG current  $I_1$ ; d: local load current  $I_{Local}$ )

The main grid voltage contains 2.8% 3rd and 2.8% 5th harmonic voltages. In this simulation, the reference power is set to 600W and 200Var. The detailed parameters of the system are provided in Table I.

When the local load harmonic current is not compensated by the DG unit (corresponding to  $I_{ref\_h} = 0$  in (15) and (16)), the performance of the DG unit is shown in Fig. 9. It can be seen from Fig. 9 (b) that the DG current is sinusoidal with 5.57% THD. At the same time, the harmonic load currents flow to the main grid is illustrated in Fig. 9 (a).

Once the local load harmonic current compensation is activated by setting  $I_{ref\_h} = I_{Local}$  in (16), the performance of the system is shown in Fig. 10. Although harmonic extractions are not used in this simulation, the proposed method can still realize satisfied local load harmonic current compensation, resulted in an enhanced grid current quality with 5.88% THD. Meanwhile, DG unit current is polluted with 201.5% THD.

For the DG unit operating under local load harmonic compensation mode, its fundamental current reference adjusted by (10) is shown in Fig. 11 (a). As the DG unit also provides 200Var reactive power to the grid, it can be seen that the fundamental current reference is slightly lagging of the PoC voltage.

The effectiveness of the proposed closed-loop power control strategy is verified in Fig. 12, where the real and reactive power is calculated by (13) and (14). When the conventional open-loop power control in (6) is applied, it can be noticed that the DG output real and reactive power control is not accurate. On the other hand, as the proposed control strategy regulates DG output power in a closed-loop manner, it guarantees zero steady-state power tracking error.

#### • Performance under frequency disturbance

The performance of the DG unit under grid voltage frequency deviation is also examined. In this test, the bandwidth ( $\omega_c$ ) of resonant controllers at harmonic frequencies is selected as 16 rad/s. As a result, the performance of current tracking can be less sensitive to grid voltage frequency variations. In Fig. 13, the DG unit power reference is

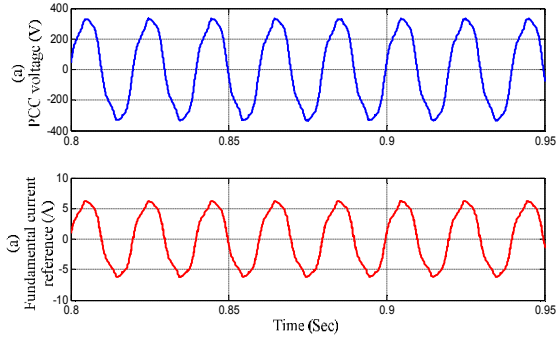


Fig. 14. PoC voltage and the fundamental current reference for DG unit during harmonic rejection. (a: PoC voltage  $V_{PoC}$ ; b: fundamental current reference  $I_{ref\_f}$ .)

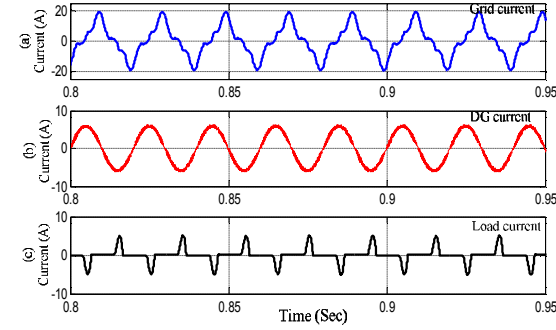


Fig. 15. Performance of the DG unit during harmonic rejection. (a: grid current  $I_2$ ; b: DG current  $I_1$ ; c: Load current  $I_{Load}$ .)

600W/600Var and the grid voltage frequency is fixed to 50Hz before 1.0 sec. During this time range, it can be seen that DG unit absorbs the harmonic current from local nonlinear loads and the grid current THD is only 5.05%.

At the time instant 1.0 sec, the grid frequency jumps to 52Hz. In the case of grid frequency variation, it can be seen that the proposed method still maintains satisfied harmonic compensation performance with 5.99% grid current THD. It is emphasized here that in a real DG system, the frequency deviation is typically lower. E.g. for the small PV systems, the allowed frequency deviation range is -0.7Hz to 0.5Hz. The DG unit needs to be disconnected from the utility when the grid frequency deviation is out of this range [35]. If very larger frequency variation is present, a frequency estimator could be used to update the PR control parameters. As discussed earlier, such a frequency estimator will be simpler than a PLL.

- Compensation of feeder resonance voltage

To verify the feasibility of the proposed method in compensating feeder resonance voltages, the DG unit is connected to the stiff main grid with five cascaded LC filters (see Fig. 2). The inductance and capacitance of each LC filter is 1mH and 25 $\mu$ F, respectively. The performance of this system is shown in Figs. 14 to 18.

The performance of the proposed controller under DG unit harmonic rejection mode ( $I_{ref\_h} = 0$ ) is given in Figs. 14 and 15. As shown in the upper part of Fig. 14, the PoC voltage is distorted with 13.6% THD, due to the resonance aggregated in the LC ladder. Since the fundamental current ( $I_{ref\_f}$ ) is

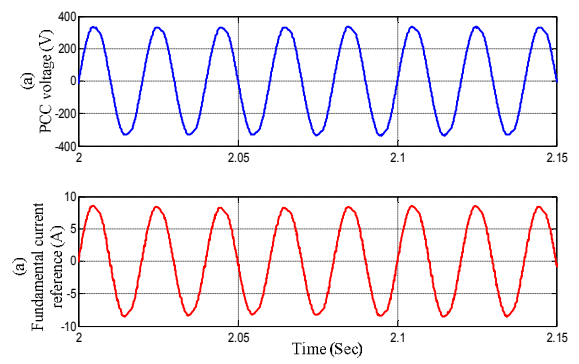


Fig.16. PoC voltage and its corresponding fundamental current reference during feeder resonance voltage compensation. (a: PoC voltage  $V_{PoC}$ ; b: fundamental current reference  $I_{ref\_f}$ .)

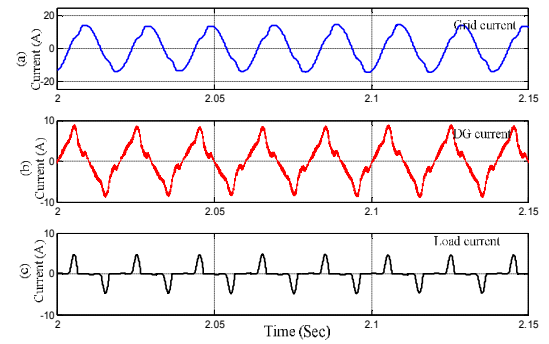


Fig.17. Performance of the DG unit during feeder resonance voltage compensation. (a: grid current  $I_2$ ; b: DG current  $I_1$ ; c: Load current  $I_{Load}$ .)

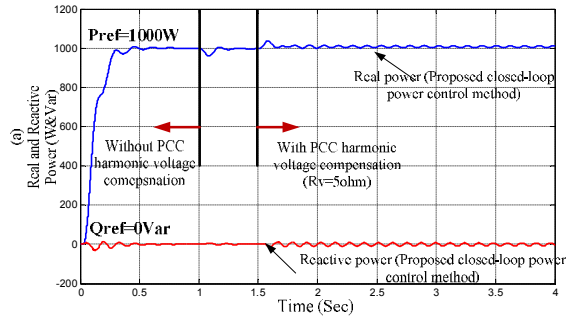


Fig.18. Power flow of the DG unit with LC ladder. ( $P_{ref}=1000W$  and  $Q_{ref}=0$  Var)

synchronized with the non-filtered PoC voltage and its orthogonal component, it is also distorted as presented in the lower part of Fig. 14.

Although the fundamental current reference derived by (10) is distorted, it can be seen from Fig. 15 (b) that the DG current is sinusoidal with 5.61% THD. Meanwhile, the main grid current contains non-trivial harmonics with 34.2% THD.

When the feeder resonance voltage compensation is enabled by controlling the DG unit as a virtual resistance ( $R_v=5$  in (16)) at selected harmonic frequencies, corresponding responses of the system are shown in Figs. 16 and 17. In

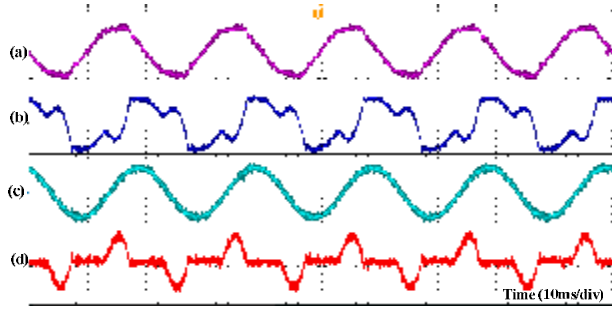


Fig.19. Performance with local nonlinear load. DG unit works under harmonic rejection mode (a: PoC voltage 250v/div; b: grid current 10A/div; c: DG current 10A/div; d: local load current 10A/div.)

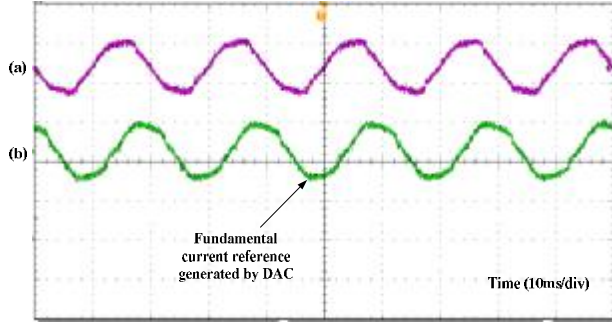


Fig.20. Performance with local nonlinear load. DG unit works under harmonic rejection mode. (a: PoC voltage 250v/div; b: fundamental current reference  $I_{ref\_f}$  10A/div.)

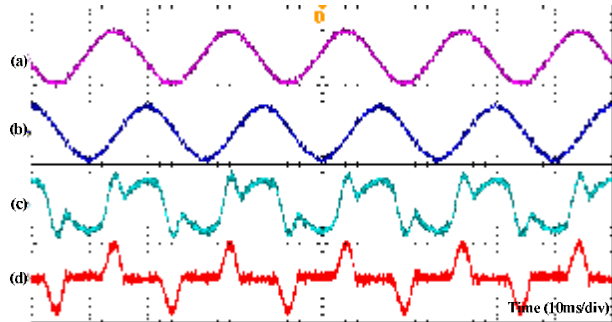


Fig.21. Performance with local nonlinear load. DG unit works under local load harmonic compensation mode. (a: PoC voltage 250v/div; b: grid current 10A/div; c: DG current 10A/div; d: local load current 10A/div.)

contrast to the performance in Figs. 14, it can be seen from Fig. 16 that the PoC harmonic voltage in this case is mitigated and its THD reduces to 3.07%.

The associated current waveforms during feeder resonance voltage compensation are shown in Fig. 17. It is obvious that DG current has more distortions (with 35.09% THD), while the main grid current THD reduces to 8.12%.

Finally, the power flow performance of the DG unit using the proposed power control scheme is shown in Fig. 18. From the time range 0 sec to 1.0 sec, the DG unit is controlled to eliminate DG harmonic currents ( $I_{ref\_h} = 0$ ). From 1.0 sec to 1.5 sec, feeder resonance voltage compensation is slowly activated by changing  $R_v$  from infinity to  $5\Omega$ . It can be seen that the power control is always accurate during the transitions between different control modes.

## B. Experimental results

Similar tests are also conducted in the laboratory prototype, where a single-phase Danfoss inverter is connected to a scaled down grid with 115V rated voltage magnitude. The real-time code for the experiment is generated by dSPACE 1005.

### • Compensation of local nonlinear loads

First, the performance of the proposed method in addressing local load harmonic is tested. The detailed system configuration and parameters can be seen from Fig. 1 and Table I, respectively. In order to absorb the switching ripple of the inverter, a small shunt capacitor ( $2\mu\text{F}$ ) is also connected at PoC.

Fig. 19 shows the performance of the DG unit operating in harmonic rejection mode, where the real and reactive power references are 200W and 500Var. Fig. 19 (b) and (c) show that the DG current is sinusoidal and the local load harmonic currents are pushed to the main grid side. In this case, the THDs of DG and grid currents are 5.16% and 41.73%, respectively. Meanwhile, due to the harmonic voltage drops on the grid feeder ( $L_g$  and  $R_g$ ), the PoC voltage is also distorted with 9.49% THD.

By using the DAC ports of dSPACE controller, the fundamental current reference during harmonic rejection operation is captured in the middle of Fig. 20. As the fundamental current reference is the combination of non-filtered PoC voltage and its conjugated component (see (10)), it is also distorted. Nevertheless, thanks to the unique feature of the proposed controller, DG current is sinusoidal.

When the DG unit works at local harmonic compensation mode, the corresponding performance of the system is shown in Fig. 21. In this experiment, the measured local load current is directly employed as the input of the harmonic control branch. It shows that the local load harmonic current are compensated by DG unit, resulted in an improved main grid current (with 3.64% THD) in Fig. 21 (b). At the same time, the DG current is polluted with 51.08% THD.

The real and reactive power control under harmonic compensation mode is also tested. To demonstrate the effectiveness of the proposed closed-loop power control method, the magnitude of main grid voltage is intentionally reduced to 106V. The performance using the proposed power control method is shown in Fig. 22, where the real and reactive power references have a step jump from 100W/250Var to 200W/500Var. It is obvious that the proposed method maintains an accurate power tracking even when the main grid voltage varies.

The power control performance using the fundamental current reference in (1) is also illustrated in Fig. 23 for comparison. In this experiment,  $E^*$  in (1) is fixed to nominal voltage magnitude 115V. In contrast to the performance using the proposed closed-loop power control, the variation of main grid voltage magnitude introduces nontrivial steady-state real and reactive power control errors.

### • Compensation of feeder resonance voltage

To evaluate the performance of the proposed method in mitigating LC ladder harmonic voltage aggregation, the DG unit is connected to the main grid with an LC ladder, which is composed of 5 identical LC filter units. The parameters of each

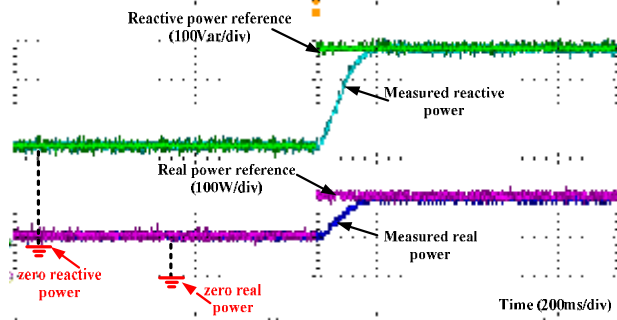


Fig.22. Real and reactive power flow using the proposed closed-loop power control method. (Under local nonlinear load compensation mode and the PoC voltage magnitude is reduced to 106V)

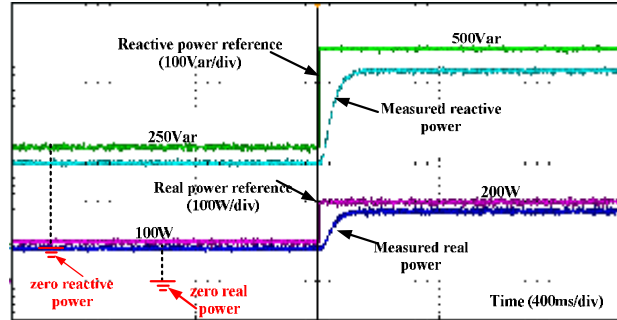


Fig.23. Real and reactive power flow using the conventional open-loop power control method in (1). (Under local nonlinear load compensation mode and the PoC voltage magnitude is reduced to 106V)

LC filter are 1mH and 25 $\mu$ F. The corresponding performances are shown in Figs. 24-27.

In the first test, the DG unit works under harmonic rejection mode. Due to the disturbance of diode rectifier at the upstream of the LC ladder (see Fig. 2), the voltages at different nodes of the LC ladder are distorted. Fig. 24 shows the waveforms of the distorted voltages. The THDs of node 1, 3, and PoC voltage are 11.46%, 14.09%, and 17.03%, respectively. It proves that feeder voltage quality is sensitive to upstream nonlinear load disturbance when the conventional DG unit without active resonance damping control is installed at the end of a feeder.

During DG harmonic current rejection operation, the fundamental current reference is shown in Fig. 25 (b). As the fundamental current is directly derived from the non-filtered PoC voltage, it is also distorted. Nevertheless, the DG current in Fig. 24 (d) is still sinusoidal with 6.02% THD.

The performance of feeder resonance voltage mitigation using virtual harmonic resistance ( $R_v$ ) is shown Figs. 26 and 27. In this case, a 5 $\Omega$  harmonic virtual resistance is used in (16). Compared to the situation using DG harmonic rejection control, the control of virtual damping resistance can effectively mitigate voltage distortions in the LC ladder, leaving an enhanced voltage quality. The voltage THDs of node1, node3, and PoC are 7.49%, 5.54%, and 5.25%, respectively.

In the case of feeder resonance voltage mitigation, the fundamental current reference as shown in Fig. 27 (b) contains less distortion as compared to the case in Fig. 25 (b). However, since the input of harmonic control branch is not zero, it can be seen that the DG current in Fig. 26 (d) is polluted with 28.25% THD.

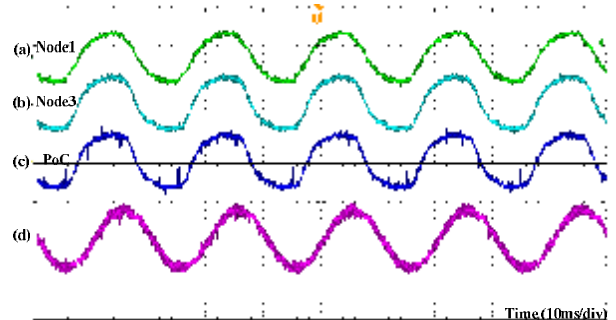


Fig.24. Performance with an upstream LC ladder. DG unit works under harmonic rejection mode. (a: node1 voltage 250v/div; b: node3 voltage 250v/div; c: PoC voltage 250v/div; d: DG current 5A/div.)

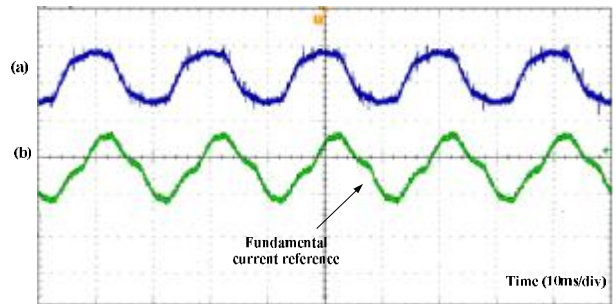


Fig.25. Performance with an upstream LC ladder. DG unit works under harmonic rejection mode. (a: PoC voltage 250v/div; b: fundamental current reference  $I_{ref\_f}$  5A/div.)

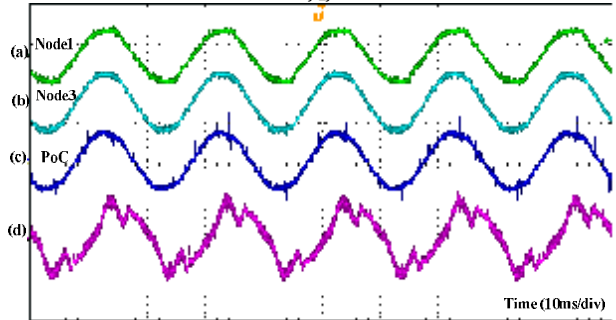


Fig.26. Performance with an upstream LC ladder. DG unit works under harmonic compensation mode. (a: node1 voltage 250v/div; b: node3 voltage 250v/div; c: PoC voltage 250v/div; d: DG current 5A/div.)

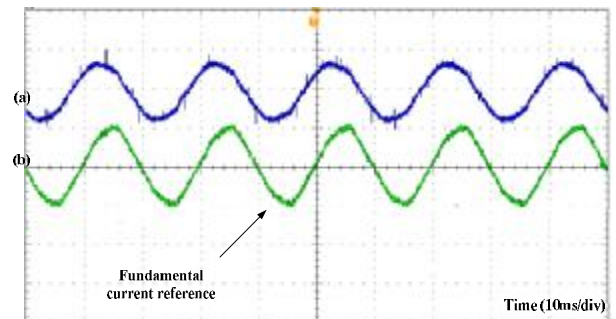


Fig.27. Performance with an upstream LC ladder. DG unit works under harmonic compensation mode. (a: PoC voltage 250v/div; b: fundamental current reference  $I_{ref\_f}$  5A/div.)

## V. CONCLUSIONS

In this paper, a simple harmonic compensation strategy is proposed for current controlled DG unit interfacing converters. By separating the conventional proportional and multiple resonant controllers into two parallel control branches, the proposed method realizes power control and harmonic compensation without using any local nonlinear load harmonic current extraction or PoC harmonic voltage detection. Moreover, the input of the fundamental power control branch is regulated by a closed-loop power control scheme, which avoids the adoption of phase-locked loops. The proposed power control method ensures accurate power control even when harmonic compensation tasks are activated in the DG unit or the PoC voltage changes. Simulated and experimental results from a single-phase DG unit verified the feasibility of the proposed strategy.

#### REFERENCES

- [1] F. Blaabjerg, Z. Chen, and S. B. Kjaer, "Power electronics as efficient interface in dispersed power generation systems," *IEEE Trans. Power Electron.*, vol. 19, pp. 1184-1194, Sep. 2004.
- [2] F. Wang, J. L. Duarte, M.A.M. Hendrix, and P. F. Ribeiro, "Modeling and analysis of grid harmonic distortion impact of aggregated DG inverters," *IEEE Trans. Power Electron.*, vol. 26, no.3, pp. 786-797, Mar. 2011.
- [3] L. Asiminoaei, F. Blaabjerg, S. Hansen, and P. Thogersen, "Adaptive compensation of reactive power with shunt active power filters," *IEEE Trans. Ind.Applicat.*, vol. 44, no. 3, pp. 867-877, May/June. 2008.
- [4] L. Asiminoaei, F. Blaabjerg, and S. Hansen, "Detection is key-harmonic detection methods for active power filter applications," *IEEE Ind. Applicat. Mag.*, vol. 13, no. 4, pp. 22-33, Jul/Aug. 2007.
- [5] N. Pogaku and T.C. Green, "Harmonic mitigation throughout a distribution system: a distributed-generator-based solution," *IEE Proc. Gener. Transm. Distrib.*, vol.153, no.3, pp. 350- 358, May. 2006.
- [6] C. J. Gajanayake, D. M. Vilathgamuwa, P. C. Loh, R. Teodorescu, and F. Blaabjerg, "Z-source-inverter-based flexible distributed generation system solution for grid power quality improvement," *IEEE Trans. Energy Conversion*, vol.24, pp.695-704, Sep. 2009.
- [7] R. I. Bojoi, G. Griva, V. Bostan, M. Guerriero, F. Farina, and F. Profumo, "Current control strategy of power conditioners using sinusoidal signal integrators in synchronous reference frame," *IEEE Trans. Power. Electron.*, vol. 20, no. 6, pp. 1402-1412, Nov. 2005.
- [8] T.-L. Lee and P.-T. Cheng, "Design of a new cooperative harmonic filtering strategy for distributed generation interface converters in an islanding network," *IEEE Trans. Power Electron.*, vol. 22, no. 5, pp. 1919-1927, Sep. 2007.
- [9] B. Han, B. Bae, H. Kim, and S. Baek, "Combined operation of unified power-quality conditioner with distributed generation," *IEEE Trans.Power Delivery.*, vol. 21, no. 1, pp. 330-338, Mar. 2003.
- [10] M. Cirrincione, M. Pucci, G. Vitale, "A single-phase DG generation unit with shunt active power filter capability by adaptive neural filtering," *IEEE Trans. Ind. Electron.*, vol. 55, no. 5, pp. 2093-2010, May. 2008.
- [11] R. I. Bojoi, L. R. Limongi, D. Roiu, and A. Tenconi, "Enhanced power quality control strategy for single-phase inverters in distributed generation systems," *IEEE Trans.Power Electron.*, vol. 26, no.3, pp. 798-806, Mar. 2011.
- [12] J. He, Y. W. Li, and S. Munir, "A flexible harmonic control approach through voltage controlled DG-Grid interfacing converters," *IEEE Trans. Ind. Electron.*, vol. 59, no. 1, pp. 444-455, Jan. 2012.
- [13] B. P. Mcgrath, D. G. Holmes, and J. J. H. Galloway, "Power converter line synchronization using a discrete Fourier transform (DFT) based on a variable sample rate," *IEEE Trans. Power Electron.*, vol. 20, no. 4, pp. 877-884, Apr. 2005.
- [14] H. Akagi, Y. Kanazawa, and A. Nabae, "Instantaneous reactive power compensation comprising switching devices without energy storage components," *IEEE Trans. Ind.Applicat.*, vol. 20, no. 3, pp. 625-630, Mar/Apr. 1984.
- [15] P. Rodriguez, A. Luna, I. Candlea, R. Mujal, R. Teodorescu, and F. Blaabjerg, "Multiresonant frequency-locked loop for grid synchronization of power converters under distorted grid conditions," *IEEE Trans. Ind. Electron.*, vol. 58, no. 1, pp. 127-138, Jan. 2011.
- [16] J. Miret, M. Castilla, J. Matas, J. M. Guerrero, and J. C. Vasquez, "Selective harmonic-compensation control for single-phase active power filter with high harmonic rejection," *IEEE Trans. Ind. Electron.*, vol. 56, no. 8, pp. 3117-3127, Aug. 2009.
- [17] D. A. Toerrey and A. M. A. M. Al-Zamel, "Single-phase active power filters for multiple nonlinear loads," *IEEE Trans. Power Electron.*, vol. 10, no. 3, pp. 263-272, May. 1995.
- [18] D. N. Zmood, D. G. Holmes, and G. H. Bode, "Stationary frame current regulation of PWM inverters with zero steady-state error," *IEEE Trans.Power Electron.*, vol. 18, pp. 814-822, Mar. 2003.
- [19] A. Timbus, M. Liserre, R. Teodorescu, P. Rodriguez, and F. Blaabjerg, "Evaluation of current controllers for distributed power generation systems," *IEEE Trans. Power Electron.*, vol. 24, no. 3, pp. 654-664, Mar. 2009.
- [20] M. Castilla, J. Miret, J. Matas, L. G. de Vicuña, and J. M. Guerrero, "Linear current control scheme with series resonant harmonic compensator for single-phase grid-connected photovoltaic inverters," *IEEE Trans. Ind. Electron.*, vol. 55, no. 7, pp. 2724-2733, Jul. 2008.
- [21] J. He and Y. W. Li, "Analysis, design and implementation of virtual impedance for power electronics interfaced distributed generation," *IEEE Trans. Ind.Applicat.*, vol. 47, no. 6, pp. 2525-2038, Nov/Dec. 2011.
- [22] Y. W. Li, D. M. Vilathgamuwa and P. C. Loh, "Design, analysis and real-time testing of a controller for multibusmicrogrid system," *IEEE Trans. Power Electron.*, vol. 19, no. 9, pp. 1195-1204, Sep. 2004.
- [23] X. Sun, J. Zeng, and Z. Chen, "Site selection strategy of single frequency tuned R-APF for background harmonic voltage damping in power systems," *IEEE Trans. Power Electron.*, vol. 28, no. 1, pp. 135-143, Jan. 2013.
- [24] C. Lascu, L. Asiminoaei, I. Boldea, and F. Blaabjerg, "High performance current controller for selective harmonic compensation in active power filters," *IEEE Trans. Power Electron.*, vol. 22, no. 5, pp. 1826-1835, May. 2007.
- [25] C. Lascu, L. Asiminoaei, I. Boldea, and F. Blaabjerg, "Frequency response analysis of current controllers for selective harmonic compensation in active power filters," *IEEE Trans. Power Electron.*, vol. 56, no. 2, pp. 337-347, Feb., 2009.
- [26] H. Akagi, "Control strategy and site selection of a shunt active filter for damping of harmonic propagation in power distribution systems," *IEEE Trans. Power Delivery.*, vol. 12, no. 1, pp. 354-363, Jan., 1997.
- [27] S. Y. Park, C. L. Chen, J. S. Lai, and S. R. Moon, "Admittance compensation in current loop control for a grid-tied LCL filter fuel cell inverter," *IEEE Trans.Power Electron.*, vol. 23, no.4, pp. 1716-1723, Jul. 2008.
- [28] M. Liserre, R. Teodorescu, and F. Blaabjerg, "Stability of photovoltaic and wind turbine grid-connected inverters for a large set of grid impedance values," *IEEE Trans. Power Electron.*, vol. 21, no. 1, pp. 263-272, Jan. 2006.
- [29] J. He, Y. W. Li, D. Bosnjak, and B. Harris, "Investigation and active damping of multiple resonances in a parallel-inverter based microgrid," *IEEE Trans. Power Electron.*, vol. 28, no. 1, pp. 234-246, Jan. 2013.

- [30] J. He and Y. W. Li, "Hybrid voltage and current control approach for DG-Grid interfacing converters with LCL filters," *IEEE Trans. Ind. Electron.*, to be published.
- [31] H. Akagi, E. H. Watanabe, and M. Aredes, "Instantaneous power theory and applications to power conditioning," *Wiley-IEEE Press*, pp.74-79, Feb. 2007.
- [32] Y. Wang and Y. W. Li, "Three-phase cascaded delayed signal cancellation PLL for fast selective harmonic detection," *IEEE Trans. Ind. Electron.*, to be published.
- [33] H. Akagi, "Control strategy and site selection of a shunt active filterfor damping of harmonic propagation in power distribution systems," *IEEE Trans. Power Deliv.*, 1997, vol. 12, no. 1, pp. 354–363, Jan. 1997.
- [34] H. Akagi, H. Fujita, and K. Wada, "A shunt active filter based onvoltage detection for harmonic termination of a radial powerdistribution line," *IEEE Trans. Ind. Appl.*, vol. 35, no. 3, pp. 638–645, May/Jun. 1999.
- [35] IEEE Recommended Practice for Utility Interface of Photovoltaic (PV) Systems, IEEE Std 929-2000, Jan. 2000.
- [36] S. G. Jorfge, C. A. Busada, and J. A. Solsona, "Frequency adaptive current controller for three-phase grid-connected converters," *IEEE Trans. Ind. Electron.*, early online access, 2013.